Journal of
MATERIALS RESEARCH

Effect of heat treatment on formation of sol-gel (Pb, La)TiO_3 films for optical application

Junmo Koo, Sung-Uk Kim, Dae Sung Yoon, Kwangsoo No, and Byeong-Soo Bae
Department of Materials Science and Engineering, Korea Advanced Institute of Science and Technology (KAIST), Taejon 305-701, Korea

(Received 26 May 1996; accepted 9 August 1996)

Lead lanthanum titanate [(Pb, La)TiO_3] sol-gel films have been prepared to investigate the effect of heat treatment on the fabrication of uniform and crack-free thick films by applying different heating schedules. The surface morphology as well as the optical properties such as refractive index, optical transmission, and optical propagation loss of the films was examined, depending on the film thickness. Because the slower and longer heating is enough to remove the organic and nitrate residues and diminish the thermal shock while heating the films, slower and longer heating can produce the uniform and crack-free thick films having higher refractive index as well as lower optical propagation loss. Also, the drying and heating of the films on a hot plate in every coating resulted in the fabrication of thick films having above 8000 Å without any defects and microcracks. This film presented the highest refractive index as well as the lowest optical propagation loss which grows exponentially with increasing the film thickness due to the scattering of defects in the film.

I. INTRODUCTION

Given the increasingly important role of integrated optics, thin film materials that are transparent and show good optically nonlinear properties are in large demand. Among the ferroelectric thin films, the lanthanum-doped lead zirconium titanate, (Pb, La)(Zr, Ti)O_3 (PLZT), thin films have been widely used in waveguide applications.[1,2] The advantages of La doping as a chemical modifier are known in several aspects: in reducing light scattering resulting from multiple refraction at the boundaries of the randomly oriented grains by reducing the distortion of the oxygen octahedral unit cell, in producing an extensive series of homogeneous solid solution compositions without any secondary phases by virtue of its high solubility in the PZT perovskite structure, in enhancing the densification process by producing a significant number of lattice vacancies, and in controlling the grain growth behavior through promoting a highly uniform microstructure. However, when an amorphous PLZT film prepared by using the sol-gel method is heat-treated, perovskite phase and undesired pyrochlore phase are simultaneously formed. The ferroelectric PLZT thin film should have higher perovskite content in order to exhibit better electro-optic properties. The composition without zirconium content [$(Pb_{1-x/100}La_x)Ti_{1-x/400}O_3$ is called PLTx] has been known to be more adequate for waveguide applications due to its finer grain size and higher transparency than PLZT.[3] Actually, the total internal reflection (TIR) optical switch was proposed and implemented using PLT28 thin films with high quadratic electro-optic coefficient.[4]

PLT thin films for optical waveguide applications must satisfy grain sizes smaller than the operating wavelength, higher refractive index than that of the substrates, thickness range between 0.2 and 1.0 μm, absence of the defects and optical inclusions, and crystallographic orientation or epitaxy.[5] In particular, thick ferroelectric films are able to make multimode waveguides because the number of modes depends on the thickness at the constant wavelength. For the optical waveguide application of ferroelectric films, a wet chemical process such as sol-gel or metal-organic decomposition (MOD) using various precursors has been used.[6,7] The advantages of this process are easier composition control, film homogeneity, easier fabrication of large area thin films, low cost, and a simple fabrication cycle. However, it is difficult to produce thick and crack-free films by this technique. The present study investigated the effect of heat treatment on the formation of thicker, crack-free, and dense sol-gel PLT films. Also, the optical propagation losses with other optical properties were measured, and the optimum heating condition was found for the application of optical waveguide.

II. EXPERIMENTAL PROCEDURE

A. Thin film preparation

The composition that was investigated in the present study is the one containing 28 mole % La in $(Pb_{1-x/100}La_x)Ti_{1-x/400}O_3$, represented by PLT28, since the lowest optical propagating loss was shown previously.[8] A precise procedure for preparing the precursor solution is shown in Fig. 1. Lead acetate [$Pb(CH_3COO)_2 \cdot 3H_2O$],

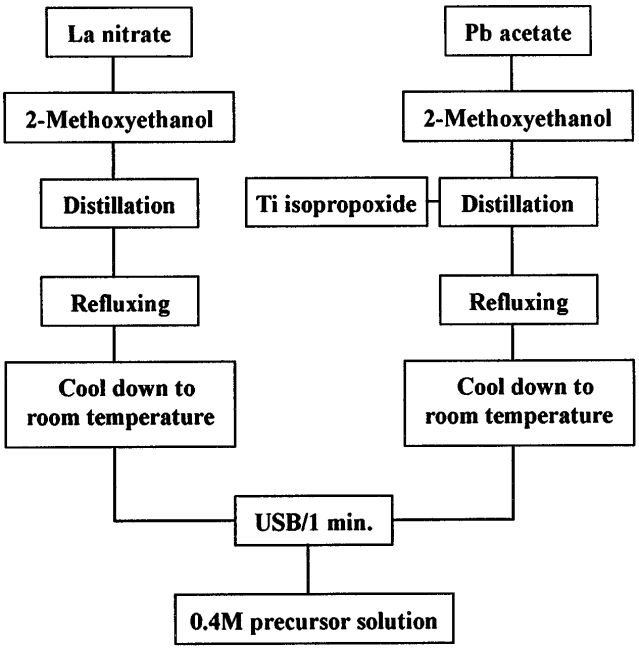

FIG. 1. Procedure of preparing PLT precursor solution.

lanthanum nitrate [$La(NO_3)_3 \cdot 6H_2O$], and titanium isopropoxide {$Ti[(CH_3)_2CHO]_4$} were used as precursors. The sol-gel PLT thin films containing large La contents have been rarely fabricated due to the low solubility of La precursors in alcohol. However, the sol-gel PLT28 thin films were successfully fabricated using lanthanum nitrate as a La precursor recently.[9,10] Also, 5 mole % excess Pb was incorporated since it was found that excess PbO aids significantly compensated PbO loss if normal stoichiometric composition were used.[11] Methoxyethanol ($CH_3OCH_2CH_2OH$) was used as a solvent to facilitate the dehydration by heating since it boils at 125 °C. Lead acetate was dissolved in methoxyethanol on heating at 120 °C for 6 h to decrease residual water, and titanium isopropoxide was then added. The solution was again heated for 6 h to be redistilled and refluxed at 80 °C for 10 h. The precursor mixture solution was then cooled down to room temperature. La solution was made with a similar process. These solutions were spin-coated on glass (Corning 7059, 20 × 20 × 0.5 mm) substrates using a spin coater (Headway Research Inc., EC101-R485) at 1500 rpm for 30 s. Then the green films were dried at 350 °C on a hot plate for 10 min, yielding about 800 Å film thickness per coating. This procedure was repeated until a desired thickness was obtained. The films were heat-treated at 520 °C with different heating schedules to densify and crystallize the films. Five different heating schedules applied to investigate the effect of heat treatment are listed in Table I. The films were inserted into the furnace which was already heated at 520 °C and maintained for 30 min (I) and 2 h (II). Also, the films were heat-treated from room temperature to 520 °C with heating rate of 15 °C/min (III) and 5 °C/min (IV), and held for 30 min. Finally, the single-coated films were heat-treated on a hot plate at 520 °C instead of in a furnace, and this was repeated in every coating (V). All the films were cooled at 2 °C/min in atmosphere to prevent cracks from thermal shock during cooling in the films.

B. Characterizations

The crystalline phase and microstructure of the films were characterized using XRD (Rigaku, D/MAX-RC) and SEM (Philips 535M), respectively. Also, SEM analysis was used to measure the thickness of the film. The optical transmission measurements of the films on the glass substrates were performed using an UV/VIS spectrophotometer (HP 8452P). In order to measure the refractive indices of the films, the envelope method and the prism coupling method were used. In the envelope method,[12,13] light is passed normal to a film, and the transmission through the film is detected as a function of wavelength by the spectrophotometer. The refractive index of the film can be calculated from the curves of transmission, T, of the extreme which envelope the spectrum. The assumption is that the substrate has a thickness several orders of magnitude larger than that of the film and has the refractive index, n_s, and absorption coefficient, $\alpha_s = 0$. Also, the index of the surrounding air is $n_0 = 1$. The following equations were used:

$$n = [N + (N^2 - n_0^2 n_s^2)^{1/2}]^{1/2}$$

$$N = \frac{n_0^2 + n_s^2}{2} + 2n_0 n_s \frac{T_{\max} + T_{\min}}{T_{\max} T_{\min}},$$

TABLE I. The heating schedules used for the preparation of the films and their optical characterizations.

Heating schedules	UV cutoff length (nm)	Refractive index at 633 nm	Waveguiding loss (dB/cm) at 633 nm
(I) Direct insertion heating at 520 °C for 30 min	337.2	2.07	8.35 (±0.5)
(II) Direct insertion heating at 520 °C for 2 h	337.1	2.13	9.30 (±0.4)
(III) Heating with 15 °C/min to 520 °C holding for 30 min	337.2	2.18	7.05 (±0.4)
(IV) Heating with 5 °C/min to 520 °C holding for 30 min	337.1	2.20	5.14 (±0.3)
(V) Heating at 520 °C on a hot plate in every coating	337.1	2.28	4.68 (±0.3)

where n is the index of a film, N is the effective index, and T_{max} and T_{min} should be measured at the same wavelength. This method also gives the dispersion of refractive indices since the refractive index is calculated at several wavelengths.

The prism coupling method[14–16] has been used to determine the refractive index of a thin, transparent, and dielectric film. In this method, the film is pressed up against the base of a prism, satisfying a thin ($\sim 1/2\lambda$) gap between the prism and the film. The setup of the prism coupling to measure the refractive index is shown in Fig. 2(a). The laser source was a He–Ne laser (MELLES GRIOT, 5 mW) and the prism in these experiments was rutile prism with right angle and symmetric shape. When a guide mode is excited, the TE modes appear on screen as vertical line shapes, and the guided-wave mode index is readily calculated from the beam input angle at which it occurs. Usually for film guiding two TE modes, a unique solution of the refractive index and the thickness of the film can be calculated, and if the thickness is already known, the index can be calculated from a single TE mode. The accuracy of measuring the coupling angle was 0.1°, which led to an accuracy of 0.001 in the refractive index.

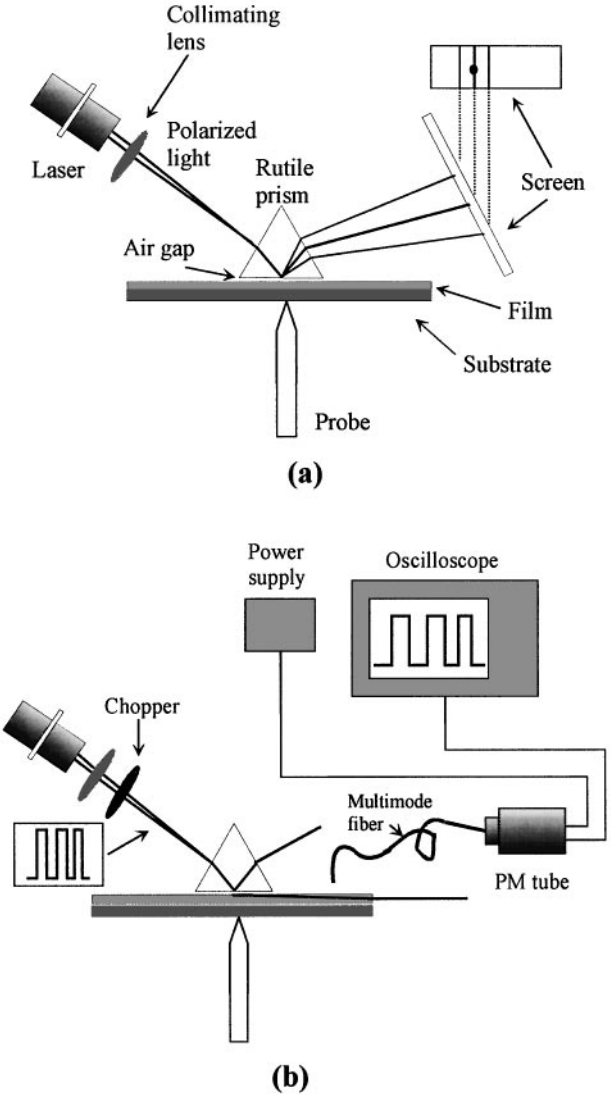

FIG. 2. Experimental setups of the prism coupler to measure (a) refractive index and (b) optical propagation loss.

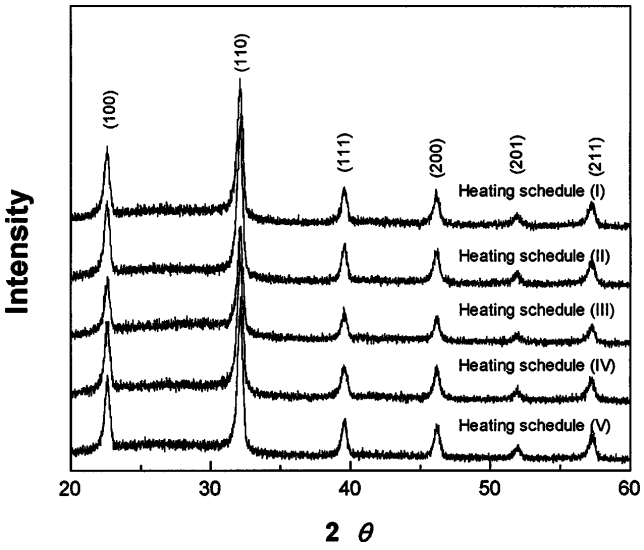

FIG. 3. XRD patterns of the films (having about 4000 Å thickness) prepared by different heating schedules.

Figure 2(b) is the setup for measuring the optical propagation losses, similar to the first setup except the chopper in front of the collimating lens and the multimode fiber to detect the intensities of guided light were used. The function of the chopper is the normalization of the signals as shown in Fig. 2(b). The optical propagation losses of the films were measured by fastening a fiber onto the surface of the film every 2.5 mm from the prism, reading the signals in the oscilloscope. The difference between the upper and lower lines of the signal in the oscilloscope indicates the intensity of guided light. The equation used to calculate the optical propagation loss, α, was

$$\alpha = |10 \cdot \log(P_1/P_2)/(L_1 - L_2)| \quad (\mathrm{dB/cm}),$$

where P_1, P_2 and L_1, L_2 are measured intensity and the distance from prism, respectively.

III. RESULTS AND DISCUSSION

A. Effect of heat treatment

The films were heat-treated at 520 °C to crystallize them to single perovskite phase with different heating schedules to investigate the effect of heat treatment. Usually, sol-gel thin films of the lead titanate based ceramics were crystallized using direct insertion heating to form single perovskite phase without pyrochlore

phase.[3] However, the direct insertion heating caused microcrack or inhomogeneities on the films due to the thermal shock and the abrupt removal of organics. Thus, in the present study, the gradual heating from room temperature was applied to obtain the uniform and crack-free single perovskite phase. Also, the green film was dried at 350 °C and heated at 520 °C on a hot plate continuously, and this drying and heating were repeated in every coating. This method can completely eliminate organics and nitrates in the films, and fabricate crack-free thick films since the volume change of the film during heating can be neglected by heating in every coating.

The XRD patterns of the films (having about 4000 Å thickness) crystallized depending on the heating schedules are shown in Fig. 3. All the films present single perovskite phase without any other noticeable phases, regardless of the heating schedules. PbO can evaporate easily in PZT composition since the partial vapor pressure of PbO is greater with increasing Zr content in the composition ($P_{PZ} > P_{PZT} > P_{PT}$).[3] Thus, the undesired pyrochlore phase is formed during heating due to the unbalanced vaporization of the constituent species in the composition. On the other hand, since the partial vapor pressure of PbO in the PLT composition is lower than that in the other compositions, such as PLZT or PZT, the stoichiometry of PLT composition can be retained to produce a single perovskite phase during any heat treatment.

The SEM micrographs of the films spin-coated 5 and 6 times (having about 4000 Å and 4800 Å thickness), crystallized with different heating schedules (I)–(IV), are shown in Figs. 4(a) and 4(b). When the films are crystallized by direct insertion heating (I and II) and fast heating (III), microcracks and nonuniformity on the surface are produced in the films. Abrupt and fast heat treatment cause the microcracks in the films due to the thermal shock during heating and remain as organic and nitrate residues in the films, making nonuniformity in the films. However, the slow heating (IV) presents the uniform, dense, and crack-free surface of the films with 5 times spin-coating (having about 4000 Å thickness), as shown in Fig. 4(a). Thus, the slow and sufficient heating to remove gradually all the organic and nitrate residues can fabricate uniform and microcrack-free films. Furthermore, even the film crystallized with slow heating (IV) is cracked and deteriorated with 6 times spin-coating (having about 4800 Å thickness), as shown in Fig. 4(b). Consequently, the slow heating can enhance the film quality, but the crack-free films over 5000 Å thickness cannot be fabricated with any heat treatment in the furnace. Figures 5(a) and 5(b) present the SEM micrographs of the films spin-coated 5 and 10 times (having about 4000 Å and 8000 Å thickness) with drying and heating on a hot plate in every coating (V). Regardless of the film thickness, the surfaces of the films are very homogeneous and crack-free. Also, the cross sections of the films show uniform film deposition without cleavages in the films, despite the respective crystallization of the film in every coating as shown in Fig. 5. When the films are coated many times and heated with heating schedules (I)–(IV), the films are shrunk suddenly since the organic and nitrate residues are evaporated at once in whole surfaces of films. Also, thermal stress owing to the thermal expansion difference between the film and the substrate is built up more and cracks the film with growing the film thickness. However, thick films above 8000 Å can be fabricated when the film is dried and heated on a hot plate in every coating since the residues and the thermal stress in the film are removed gradually in every heat treatment on a hot plate.

B. Optical characterization

The optical transmissions of the films (having about 4000 Å thickness) fabricated by different heating schedules are shown in Fig. 6(a). The UV cutoff wavelengths of the films which were listed in Table I are the same regardless of heating schedules. Thus, the surface morphology and the existence of organic and nitrate residues in the films do not have an effect on the optical transmissions of the films. However, the optical transmissions of the films prepared using heating schedule (V) with various coating numbers present the change in the UV absorption edge, as shown in Fig. 6(b). The initial increase in the film thickness shifts the UV absorption edge into longer wavelength. However, the UV absorption edge of the films does not change with more increasing in the film thickness after 7 times coating, depending on the film thickness. The initial increase in the film thickness enhances the crystallization in the films, moving the UV absorption edge into longer wavelength. On the other hand, more growth of the film thickness over the critical film thickness makes the film bulky, balancing the transmission and UV absorption at the internal faces of the films.

The refractive indices of the films measured using a prism coupler are listed in Table I. The refractive index of the film prepared by slower heating (IV) is higher than those of the films prepared by fast heating (III), and direct insertion heating (I) and (II). Also, the longer heating time for direct insertion heating resulted in the higher refractive index of the film. In spite of having the same composition as PLT28, the difference in the refractive index is attributed to the change in structural density caused by different heating schedules. The slower and longer heating enhances the crystallization and densification by removing the organic and nitrate residues in the films, producing the higher refractive indices of the films. Thus, the drying and heating in every coating (V) provides sufficient removal time and thermal energy for the film to be a dense structure, creating

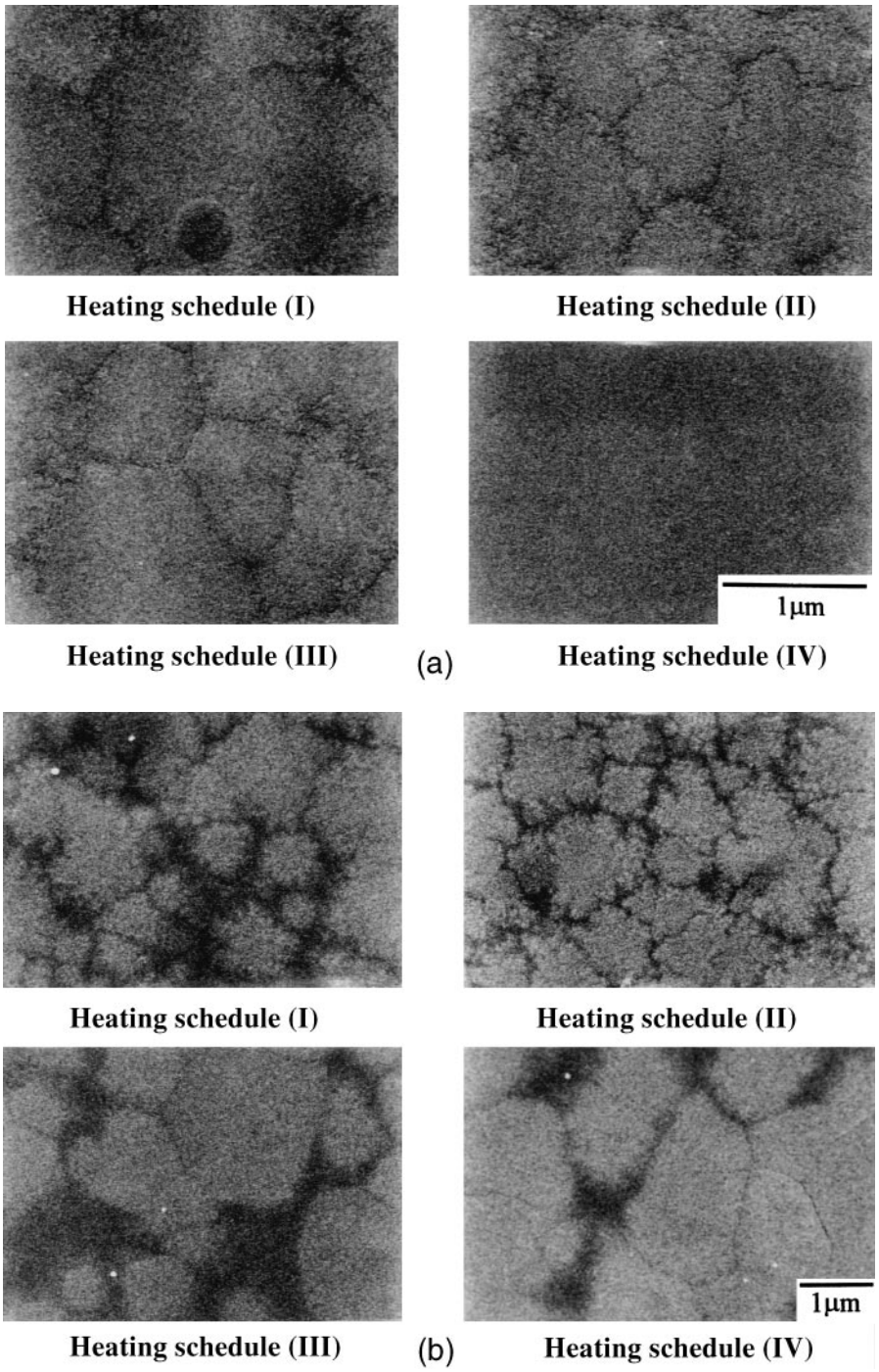

FIG. 4. Surface morphologies of the films having (a) 4000 Å and (b) 4800 Å thicknesses prepared by different heating schedules.

the highest refractive index of 2.28. These values of the refractive indices were similar to those of the films prepared by other techniques that have been reported elsewhere.[4,17,18]

Using the prism coupling method to measure the refractive index and the propagation losses, two TE modes were excited for a unique solution of the refractive index and the film thickness when the thickness of the film was usually above 4000 Å in the present study. Careful attention is needed to observe TE modes on the screen because the roughness and particles of the surface of film prevent TE modes from being excited. The measured optical propagation losses of the films prepared by different heating schedules are listed in Table I. As shown in the variation of the refractive index of the films depending on the heating schedules, the

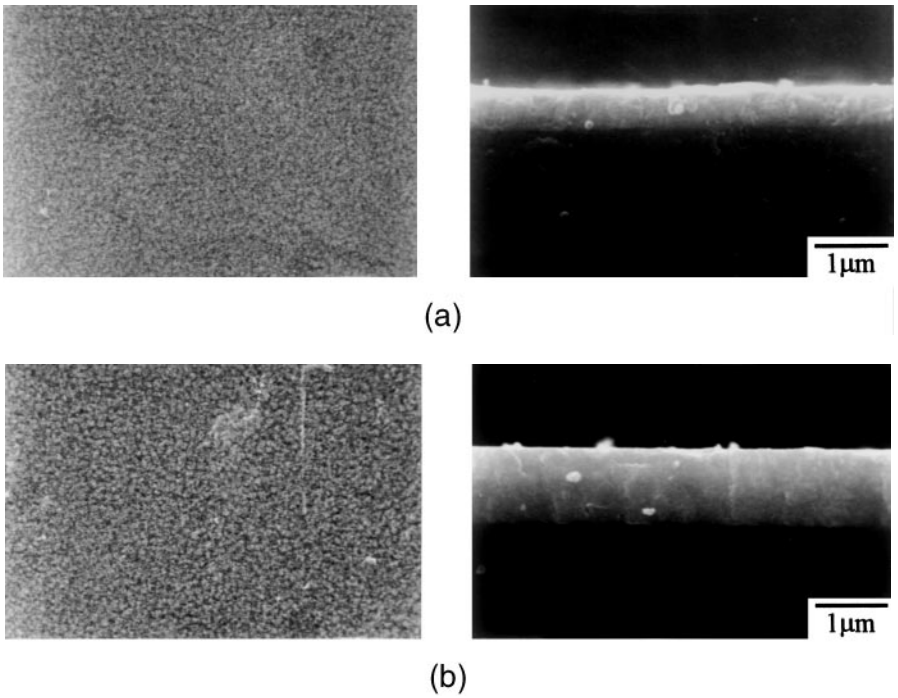

FIG. 5. Surface morphologies and cross sections of the films with (a) 4000 Å and (b) 8000 Å thicknesses prepared by the heating schedule (V).

slower and longer heating produces lower waveguiding loss due to the elimination of scattering defects such as pores, microcracks, and organic and nitrate residues in the films. Thus, the lowest waveguiding loss of 4.68 dB/cm is obtained in the film prepared by heating schedule (V) since the most uniform surface and the most densification in the films is created as discussed before. Also, the optical propagation losses of the films prepared by heating schedule (V) were plotted as a function of the coating number as shown in Fig. 7. The propagation loss increases exponentially upon growing the film thickness, although the surface roughness of the films is not greatly affected by the film thickness as shown in Fig. 5. The optical propagation loss mechanisms of the thin films include absorption, leakage, internal scattering, surface scattering, and interface scattering. Among those mechanisms, the scattering losses have been known as the most significant mechanism.[19] The surface scattering is affected by the roughness of the surface, and the internal and interface scattering is affected by the defects, depending on the film thickness. Greater roughness of the surface and the formation of the interface due to

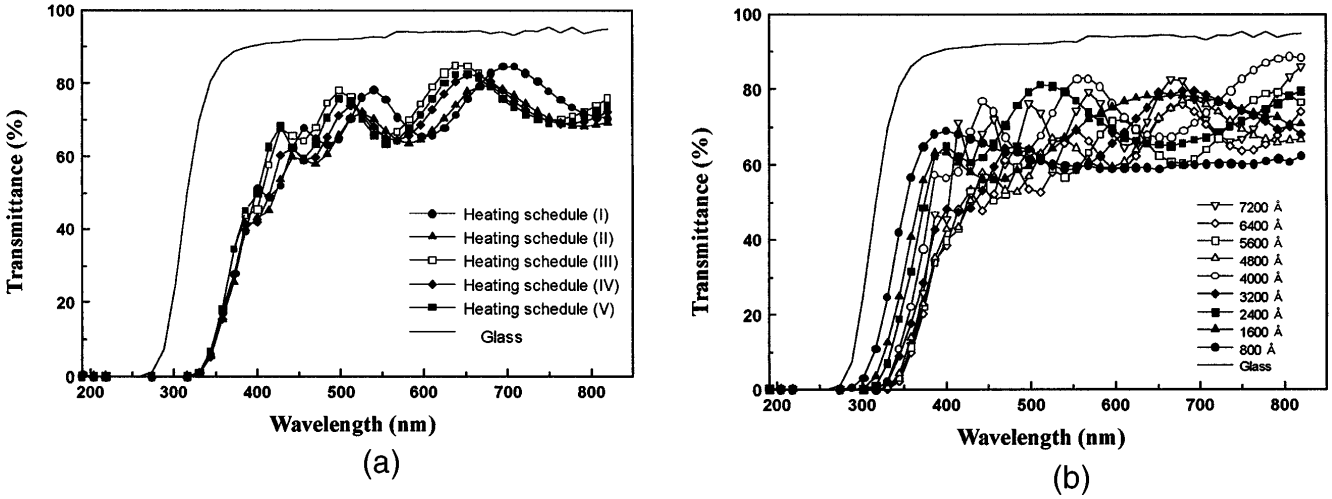

FIG. 6. Optical transmissions of the films prepared by (a) different heating schedules and with (b) various coating numbers.

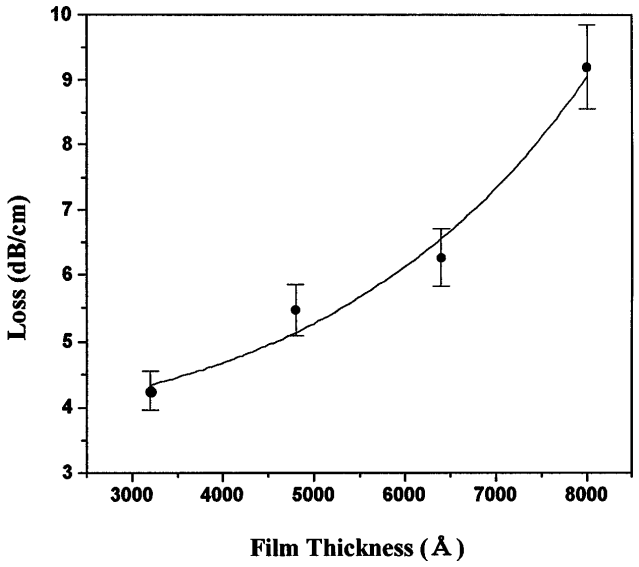

FIG. 7. Optical propagation losses of the films prepared by heating schedule (V) as a function of coating number.

the multiple coatings with increasing the film thickness may cause the enhancement of the propagation loss. However, the main mechanism of the exponential growth of the propagation loss upon increasing the film thickness can be the internal scattering due to the unavoidable defects inside the sol-gel film rather than the surface and interfacial scatterings in the film.

IV. CONCLUSION

The heat treatment to fabricate the PLT sol-gel thin film significantly affects the microstructure and optical properties of the film. All the films present single perovskite phase regardless of the heating conditions. However, the microstructure and optical properties of the films were greatly dependent upon the heating schedules. The slower and longer heating produced the uniform and crack-free surfaces of the films having up to 4000 Å thickness. Also, the densification and sufficient removal of organic and nitrate residues by sufficient heat treatment produce high refractive indices as well as low optical propagation losses of the films. Furthermore, the heating technique to dry and heat the films on a hot plate in every coating can fabricate the uniform and crack-free surface of the films having above 8000 Å thickness. Thus, the highest refractive index of 2.28 as well as the lowest waveguiding loss of 4.68 dB/cm is obtained for the film prepared by this heating method. The propagation loss of the film increases exponentially with increasing the film thickness due to the scattering by the defects in the film.

ACKNOWLEDGMENT

This work has been supported by Korea Science and Engineering Foundation (Grant No. 94-0300-06-01-3).

REFERENCES

1. G. H. Haertling, Integrated Ferroelectrics **3**, 207 (1993).
2. H. Adachi, J. Appl. Phys. **60**, 2, 736 (1986).
3. G. Teowee, Ph.D. Thesis, The University of Arizona, Tucson, AZ (1992).
4. H. Higashino, T. Kawaguchi, H. Adachi, T. Makino, and O. Yamazaki, Jpn. J. Appl. Phys. **24**, 2, 284 (1985).
5. G. Teowee, J. M. Boulton, and D. R. Uhlmann, in *Better Ceramics Through Chemistry V*, edited by M. J. Hampden-Smith, W. G. Klemperer, and C. J. Brinker (Mater. Res. Soc. Symp. Proc. **271**, Pittsburgh, PA, 1992), p. 345.
6. R. W. Vest and J. Xu, Ferroelectrics **93**, 21 (1989).
7. P. Sun, L. Zhang, and X. Yao, edited by M. Liu, A. Safari, A. Kingon, and G. Haertling (8th IEEE Int. Symp. Proc., Ferroelectrics, Greenville, SC, April 1992), p. 432.
8. G. Teowee, J. M. Boulton, S. Motakef, D. R. Uhlmann, B. J. J. Zelinski, R. Zanoni, and M. Moon, SPIE **1758**, 236 (1992).
9. Y. Liu, W. Ren, J. H. Qiu, L. Y. Zhang, and X. Yao, Ferroelectrics **152**, 195 (1993).
10. D. S. Yoon, S. U. Kim, J. Koo, Z-T. Jiang, B-S. Bae, W. J. Lee, K. No, and S. H. Cho, Kor. J. Ceram. **1**, 4 (1995).
11. V. E. Wood, J. R. Busch, S. D. Ramamurthi, and S. L. Swartz, J. Appl. Phys. **71**, 9 (1992).
12. R. Swanepoel, J. Phys. E; Sci. Instrum. **16**, 1214 (1983).
13. K. A. Epstein, D. K. Misemer, and G. D. Vernstrom, Appl. Opt. **26** (2), 294 (1987).
14. R. Ulrich and R. Torge, Appl. Opt. **12** (12), 2901 (1973).
15. P. K. Tien, R. Ulrich, and R. J. Matin, Appl. Phys. Lett. **14** (9), 291 (1969).
16. P. K. Tien and R. Ulrich, J. Opt. Soc. Am. **60** (10), 1325 (1970).
17. M. Okuyama, T. Usuki, Y. Hamakawa, and T. Nakagawa, Appl. Phys. **21**, 339 (1980).
18. D. A. Tossell, J. S. Obhi, N. M. Shorrocks, and R. W. Whatmore (ISAF IEEE Int. Symp. on the Appl. of Ferroelectrics, Sep. 1992).
19. D. K. Fork, F. Armani-Leplingard, J. J. Kingston, and G. B. Anderson, in *Thin Films for Integrated Optics Applications*, edited by B. W. Wessels, S. R. Marder, and D. M. Walba (Mater. Res. Soc. Symp. Proc. **392**, Pittsburgh, PA, 1995), p. 189.